J. Cent. South Univ. (2015) 22: 3830−3836
DOI: 10.1007/s11771-015-2927-6

Springer

Thermo-mechanical properties of bowl-shaped grinding wheel and machining error compensation for grinding indexable inserts

ZHANG Xiang-lei(张祥雷), YAO Bin(姚斌), CHEN Bin-qiang(陈彬强),
SUN Wei-fang(孙维方), WANG Meng-meng(王萌萌), LUO Qi(罗琪)

Department of Mechanical and Electrical Engineering, School of Physics and Mechanical & Electrical Engineering, Xiamen University, Xiamen 361005, China

Abstract: In order to meet the technical requirements of grinding the circumferential cutting edge of indexable inserts, thermo-mechanical properties of bowl-shaped grinding wheel in high speed grinding process and the influence of dimension variations of the grinding wheel on machining accuracy were investigated. Firstly, the variation trends of the dimension due to centrifugal force generated in different wheel speeds were studied and the effect of stress stiffening and spin softening was presented. Triangular heat flux distribution model was adopted to determine temperature distribution in grinding process. Temperature field cloud pictures were obtained by the finite element software. Then, dimension variation trends of wheel structure were acquired by considering the thermo-mechanical characteristic under combined action of centrifugal force and grinding heat at different speeds. A method of online dynamic monitoring and automatic compensation for dimension error of indexable insert was proposed. By experimental verification, the precision of the inserts satisfies the requirement of processing.

Key words: bowl-shaped grinding wheel; thermo-mechanical properties; indexable insert; machining accuracy; compensation

1 Introduction

Manufacturing errors due to grinding forces and thermal deformations account for 40%−70% in precision grinding [1]. There has been extensive research conducted about the influence of grinding force and grinding heat on machining accuracy [2−5]. However, studies on manufacturing errors due to centrifugal force, stress stiffening and spin softening in high wheel speed are rarely seen at present. Many researches focus on centrifugal force generated by spindle unit [6], turbine blade [7] and bearing [8−9], etc, however, many of them do not take into account the influence of stress stiffening and spin softening. Numerous scholars center on simulation of the single abrasive grain grinding without considering the influence of thermo-mechanical characteristic on manufacturing accuracy [10]. Grinding wheel is not only subjected to centrifugal force, stress stiffening and spin softening but also grinding heat in actual grinding. Therefore, the decrease of manufacturing accuracy due to deformations generated by thermo-mechanical action should not be neglected. It is essential to monitor and reduce the manufacturing errors due to deformations. In order to meet the requirement of accuracy in precision grinding of indexable inserts, it is vital to conduct effective detection. Generally speaking, the measurement accuracy is one order of magnitude higher than manufacturing accuracy. In order to guarantee high precision, online detection and error compensation are necessary. As for the machining error of indexable inserts, there are two basic approaches for error reduction: error avoidance and error compensation. The error avoidance method tries to eliminate possible sources of errors through design and manufacturing efforts. Improving machine tool accuracy by careful design and manufacturing has been extensively used. The error compensation methods involve the mapping of machine errors and then correcting for the effect of the errors [11−12].

Cemented carbide indexable inserts have been widely used in high efficiency and high precision computer numerical control (CNC) machine due to its high repeat positioning accuracy, rapid transferring, short auxiliary time of changing the cutting edge, etc. A diamond bowl-shaped grinding wheel is usually used to machine cemented carbide inserts in face grinding. The structure of bowel-shaped grinding wheel tends to deflect in high rotating speed compared to common wheel, which directly influences the accuracy of machining

Foundation item: Project(2010ZX04001-162) supported by the National Science and Technology Major Project of China
Received date: 2014−09−26; **Accepted date:** 2014−11−15
Corresponding author: YAO Bin, Professor, PhD; Tel: +86−592−2186923; E-mail: yaobin@xmu.edu.cn

inserts. This work aims to achieve high precision grinding for indexable inserts. A finite element model of bowl-shaped grinding wheel was built. Dimension variations of inserts under the combination of centrifugal force, stress stiffening, spin softening and grinding heat were analyzed. Further, the influence of thermo-mechanical action on machining accuracy was investigated. A method of dynamic online monitoring and machining error compensation was also proposed and verified in this work.

2 Thermo-mechanical properties of bowl-shaped grinding wheel

The bowl-shaped grinding wheel is shown in Fig. 1. The outer diameter is 400 mm, the inter diameter is 380 mm, the axial width of the wheel is 180 mm, the grinding face width is 10 mm, and the abrasive thickness is 5 mm.

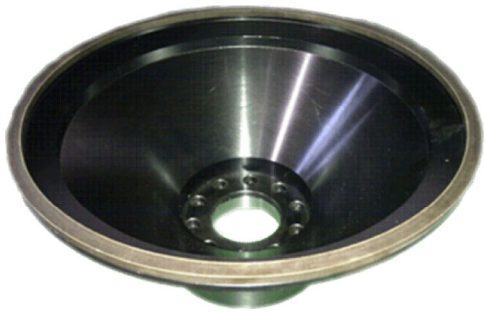

Fig. 1 Diamond bowl-shaped grinding wheel

2.1 Centrifugal force, stress stiffening and spin softening

The structure of bowl-shaped grinding wheel is axial symmetric, and it can be regarded as an aggregation structure composed of changeable hollow disks in radius and thickness. When the wheel rotates, it expands under the action of centrifugal force. Its end section is hollow rotating disk, as shown in Fig. 2. Assuming there are no

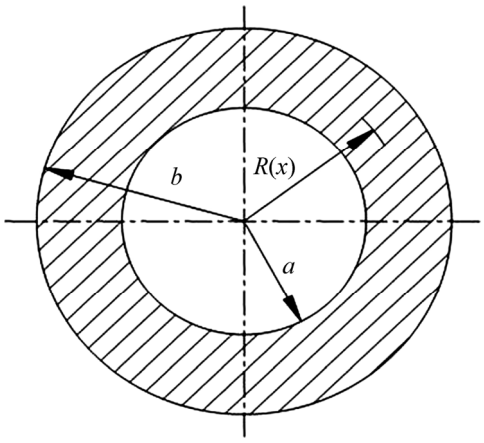

Fig. 2 End section diagram of bowl-shaped grinding wheel

surface forces in the inner hole and the outer boundary of the disk, the strain component of the end section of the wheel is given as [13−14]

$$\varepsilon_\theta = \frac{3+v}{8E}\rho\omega^2 r\left[(1-v)(b^2+a^2)+(1+v)\frac{a^2b^2}{r^2}-\frac{1-v^2}{3+v}r^2\right] \tag{1}$$

$$\varepsilon_r = \frac{3+v}{8E}\rho\omega^2 r\left[(1-v)(b^2+a^2)-(1+v)\frac{a^2b^2}{r^2}-\frac{3(1-v^2)}{3+v}r^2\right] \tag{2}$$

where a and b are the inside and outside diameters of the wheel end section, r is the radius, v is Poisson ratio, ρ is the density, ω is the angular velocity, and E is the elastic modulus. Assuming that the wheel along the axial is x coordinate, the radial deformations can be expressed as

$$u_{(x)} = \frac{3+v}{8E}\rho\omega^2 r_{(x)}\left[(1-v)(b^2+a^2)+(1+v)\frac{a^2b^2}{{r_{(x)}}^2}-\frac{1-v^2}{3+v}{r_{(x)}}^2\right] \tag{3}$$

The preload of the wheel caused by centrifugal force during the high rotating speed leads to stress variation and stiffness variation. Meanwhile, deformations of the wheel in different levels are generated because of centrifugal force, which results in stiffness decrease. The stiffness decrease due to the deformation is called spin softening [15]. Therefore, the different rotating speeds of grinding wheel generate not only different centrifugal forces but also the stress stiffening and spin softening, which leads to the change of stiffness and stress of the wheel. Finite element simulation (FEM) analysis is presented on the issue as follows.

The 3D FEM model of bowl-shaped grinding wheel is built. The dimension of the wheel is the same as mentioned above. The material properties of the grinding wheel are listed in Table 1. The 3D solid mesh elements are generated by sweeping meshing, restrictions is imposed on the contact faces and global angular velocity is loaded. The maximum line velocity of the wheel is 120 m/s. Figure 3 shows the simulation results of maximum geometry deformation and stress of the wheel caused by the centrifugal force at different rotating speeds. The simulation results considering the impact of the stress stiffening and spin softening are presented in Fig. 4. The results show that the maximum deformation and maximum stress of the wheel increase nonlinearly

Table 1 Material properties of bowl-shaped grinding wheel

Material	Elastic modulus/ GPa	Poisson ratio	Density/ (kg·m^{-3})
40Cr	210	0.28	7870

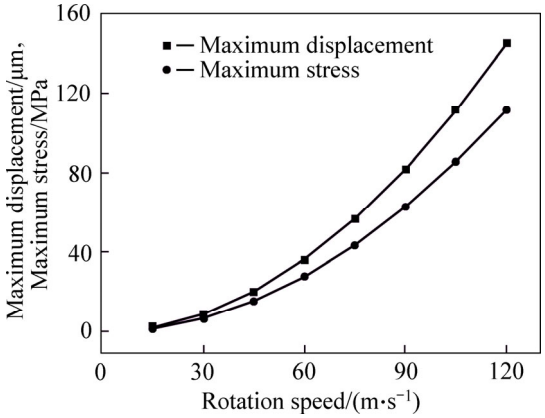

Fig. 3 Maximum displacement and stress under different rotation speeds

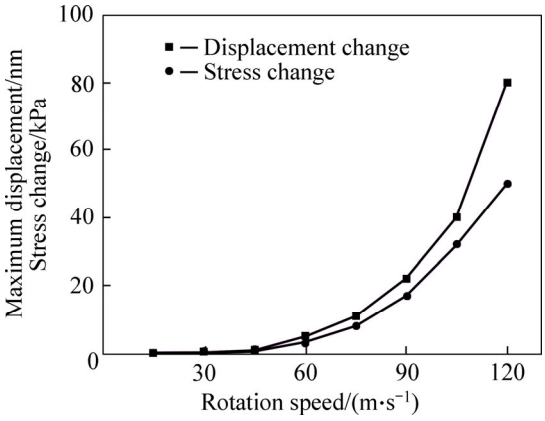

Fig. 4 Maximum displacement and stress considering stress stiffening and spin softening

with the rotating speed under centrifugal force, as well as the stress stiffening and spin softening. This means that stress stiffening is predominant compared with spin softening. Consequently, for precision grinding of indexable inserts, it is necessary to compensate the deformation error of the wheel in the NC tool path calculation.

2.2 Grinding heat of bowl-shaped grinding wheel

Friction and cutting deformation are the predominant factors for grinding heat [16]. Essentially, grinding process is a comprehensive result caused by the sliding, ploughing and cutting with a large number of irregular abrasive grains of discrete distribution on the grinding wheel surface. In actual grinding process, the indexable insert needs to be clamped just one time, and then all flanks could be ground, so the cutting depth is deeper and contact length is larger than in general conditions. Since cutting force of the abrasive grains increases gradually from run-in to run-out, using strip heat source distribution model is more reasonable. According to grinding heat source theoretical model proposed by J C Jaeger [17], assuming the grinding area heat flux is q and moving velocity is v, the temperature field is produced [17]:

$$T(x,z)=\int_{-\frac{l_c}{2}}^{\frac{l_c}{2}}\frac{q}{\pi\lambda}\exp\left[\frac{v(x-l_i)}{2\alpha}\right]K_0\left\{\frac{v[(x-l_i)^2+z^2]^{1/2}}{2\alpha}\right\}\mathrm{d}l_i \tag{4}$$

where K_0 is the Bessel function, λ is the thermal conductivity, α is the thermal diffusivity, c is the specific heat and the integral variable l_i represents the position of the heat source. Plug the initial conditions of z=0 into Eq. (4), and it is obtained:

$$T(x,0)=\frac{2q\alpha}{\pi\lambda V_{\mathrm{w}}}[\pi(l_{\mathrm{c}}-2x)]^{1/2} \tag{5}$$

When $x=-l_{\mathrm{c}}/2$, namely the heat source is close to the remove end, $T(x, 0)$ is the maximum:

$$T(x,0)=\frac{4q\alpha}{\lambda V_{\mathrm{w}}}\left(\frac{l_{\mathrm{c}}}{2\pi}\right)^{1/2} \tag{6}$$

where heat q is obtained using the Outwater and Shaw method [18]. They claim that the mechanical energy can convert into heat energy in the grinding process, so heat energy Q_{T} is calculated as follows:

$$Q_{\mathrm{T}}=F_{\mathrm{t}}(V_{\mathrm{s}}+V_{\mathrm{w}}) \tag{7}$$

where F_{t} is the tangential grinding force, V_{s} is the speed of grinding feed rate, V_{w} is the moving speed of heat source. Because V_{w} is far up to V_{s}, V_{s} can be neglected:

$$q=\beta Q_{\mathrm{T}}/A \tag{8}$$

where β is the heat rate of incoming workpiece, which can be calculated according to the heat distribution ratio model of GUO and MALKIN [19], and A is the area of grinding contact zone.

It needs less time to reach the highest temperature during high speed grinding process, generally only a few percents of a second. This is because that the movement speed of heat source is greatly high. The 3D wheel model is built and has X, Y, Z three directions, considering the cooling fluid and convective heat transfer in air medium. The model meets the instantaneous temperature field model as [20]

$$\rho c\frac{\partial\theta}{\partial t}-\frac{\partial}{\partial x}\left(k_x\frac{\partial\theta}{\partial x}\right)-\frac{\partial}{\partial y}\left(k_y\frac{\partial\theta}{\partial y}\right)-\frac{\partial}{\partial z}\left(k_z\frac{\partial\theta}{\partial z}\right)-\rho Q=0 \tag{9}$$

In the finite element simulation process of grinding temperature, the complex boundary conditions should be simplified to reduce the computation time. In the model, the workpiece is a cemented carbide indexable insert, and the wheel speed is 120 m/s. Grinding heat quickly

dissipates on grinding face of the wheel, so the heat source is simplified as a surface load (heat flow density). Meanwhile, the convective heat transfer coefficient is applied on the surface of the wheel in order to simulate the heat taken away by cooling liquid and air. The simulation results about transient temperature contour and transient thermal deformation contour after grinding for 40 s are shown in Figs. 5 and 6. Figure 7 shows the curve of temperature rise in the end face during 40 s.

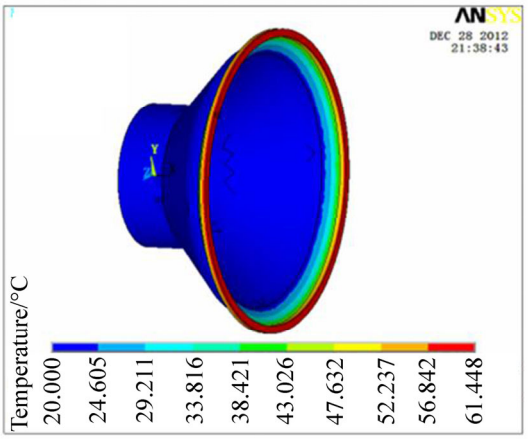

Fig. 5 Transient temperature contour of bowl-shaped grinding wheel after grinding for 40 s

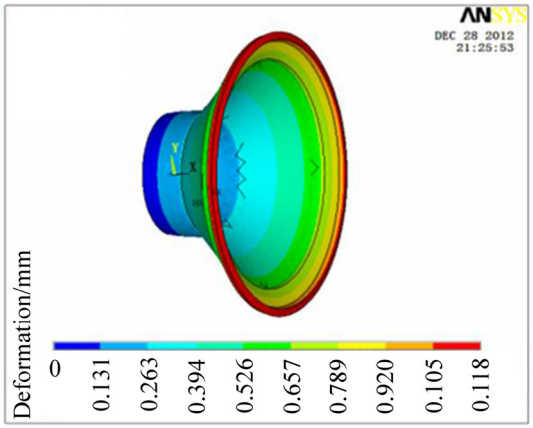

Fig. 6 Transient thermal deformation contour of bowl-shaped grinding wheel after grinding for 40 s

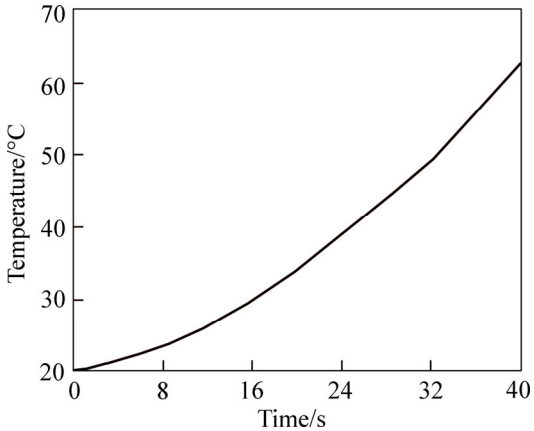

Fig. 7 Curve of temperature rise in end face

3 Thermo-mechanical analysis of bowl-shaped grinding wheel

Based on the above analysis, a coupled thermo-mechanical equation comprehensively considering speed, centrifugal force and grinding heat is built by the thermo elastic constitutive equation. The variation principle is applied. The finite element matrix equation is obtained [20]:

$$\begin{bmatrix} \boldsymbol{M} & 0 \\ 0 & 0 \end{bmatrix} \begin{Bmatrix} \ddot{u} \\ \ddot{T} \end{Bmatrix} + \begin{bmatrix} \boldsymbol{C} & 0 \\ \boldsymbol{C}^{\mathrm{tu}} & \boldsymbol{C}^{\mathrm{t}} \end{bmatrix} \begin{Bmatrix} \dot{u} \\ \dot{T} \end{Bmatrix} + \begin{bmatrix} \boldsymbol{K} & \boldsymbol{K}^{\mathrm{ut}} \\ 0 & \boldsymbol{K}^{\mathrm{t}} \end{bmatrix} \begin{Bmatrix} u \\ T \end{Bmatrix} = \begin{Bmatrix} \boldsymbol{F} \\ \boldsymbol{Q} \end{Bmatrix} \tag{10}$$

where $\boldsymbol{M}$ is the structure mass matrix, $\boldsymbol{F}$ is the force vector, $\boldsymbol{Q}$ is the heat flow vector, $\boldsymbol{K}^{\mathrm{t}}$ and $\boldsymbol{K}^{\mathrm{ut}}$ are the unit matrixes of diffusion coefficient and thermal elastic stiffness, $\boldsymbol{C}^{\mathrm{tu}}$ and $\boldsymbol{C}^{\mathrm{t}}$ are the unit matrixes of thermal elastic damping and heat capacity, and $\boldsymbol{T}$ is the temperature vector.

Thermal-mechanical analysis of bowl-shaped grinding wheel is adopted based on the sequential coupling method, the element type of temperature field analysis is Solid90, and the element type of thermal deformation analysis transforms into structural unit of Solid186. Assume that the initial temperature is 20 °C, and grinding time is 40 s. The displacement deformation and stress of the wheel caused by the action of centrifugal force and grinding heat at the highest speed (120 m/s) are analyzed, and the result is shown in Fig. 8.

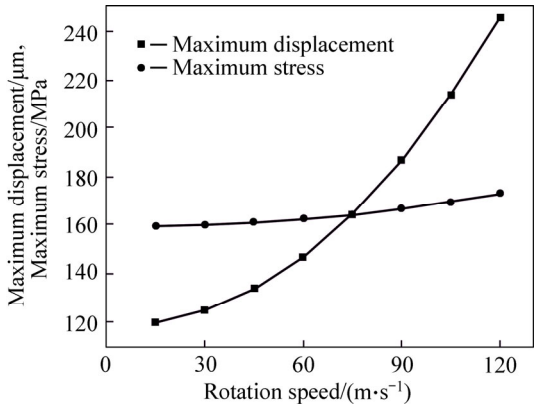

Fig. 8 Thermal mechanical coupled analysis result

As can be seen from Fig. 8, the maximum displacement and stress values of the wheel increase nonlinearly with the wheel speed increasing, and the biggest displacement value achieves up to 248 μm. As can be seen from Fig. 7, the wheel structure expands backward along the axial direction. The largest displacement occurs on the end face of the wheel. The deformation leads to a larger distance between the grinding wheel face and the insert. Since the insert profile is directly ground by the grinding wheel, the displacement of end face directly affects the machining

accuracy of inserts.

4 Dynamic monitoring and automatic compensation method for grinding indexable inserts

For grinding machining accuracy, as long as the bowl-shaped grinding wheel end face can be monitored within an expected expansion range, the consistency of inserts sizes can be controlled in the error tolerance range by compensation. By combining with the thermo-mechanical coupled properties of bowl-shaped grinding wheel, CNC system and high precision measurement system, this work presents a simple and practical method of dynamic monitoring and automatic compensation for insert machining dimension errors.

4.1 Indirect method on dynamic monitoring insert machining error instead of deformation of bowl-shaped grinding wheel

When the bowl-shaped grinding wheel gets backward extension under the effect of thermal-mechanical effect, the wheel structure occurs radial increase and axial shrink. The radial increase will not affect the machining accuracy because the edge of the insert is still in the grinding area in this situation. While, axial shrink will lead to the movement of the end face corresponding to the original location, which will affect the dimension of finished insert. As shown in Fig. 9, SPECTO3087 with contact probe of Heidenhain is used to online measure the inscribed circle diameter of the finished insert.

The measured data are linear displacements which need to be converted to the offset values between inscribed circle radius of the indexable insert and the center of clamping position. The error compensation accuracy largely depends on the calculation accuracy of the offset value. The details of the calculation can be found in Ref. [21]. Reshaping program in the machine tool is used to compensate the offset value. For the same insert, the initial offset value is large due to thermo-mechanical effect leading to backward expansion of the wheel. The offset value will be corrected by regrinding, which can reduce the waste of inserts.

4.2 Verify deformation and automatic compensation for insert machining error

When the same batch of indexable inserts is ground, the grinding speed is generally fixed. Therefore, the effect of centrifugal force, rotation softening and stress stiffening on the bowl-shaped grinding wheel is determined. After test-grinding a piece of insert and comparing processing error with theoretical size, it is shown that the error mainly results from the axial deformation of the wheel. When the wheel speed is 2000 r/min and the inserts are ground without error compensation, the error range of the inserts is (20±5) μm. The value is consistent with the theoretical deformation value of the wheel in Fig. 3, which has verified the accuracy of the theory. Therefore, bowl-shaped wheel deformation caused by the centrifugal force, rotation softening and stress stiffening can be compensated by adjusting the feed rate with the error value.

The effects of thermo-mechanical characteristic on the displacement changes of bowl-shaped grinding wheel are non-linear, and it changes with the variation of wheel speed and grinding heat. Inscribed circle diameter of each indexable insert is measured by the monitoring system to get the actual value (d_r). The error (e) is defined as the deviation between the actual value (d_r) and the nominal value (d_n). If e is within 0.01 mm, it is considered to be in the normal range of error, and the error does not need to be compensated. If e exceeds 0.01 mm, the compensation value (x) can be obtained according to

$$\begin{cases} x = \xi \cdot (d_r - d_n), & e > 0.01 \text{ mm} \\ x = 0, & e \le 0.01 \text{ mm} \end{cases} \tag{11}$$

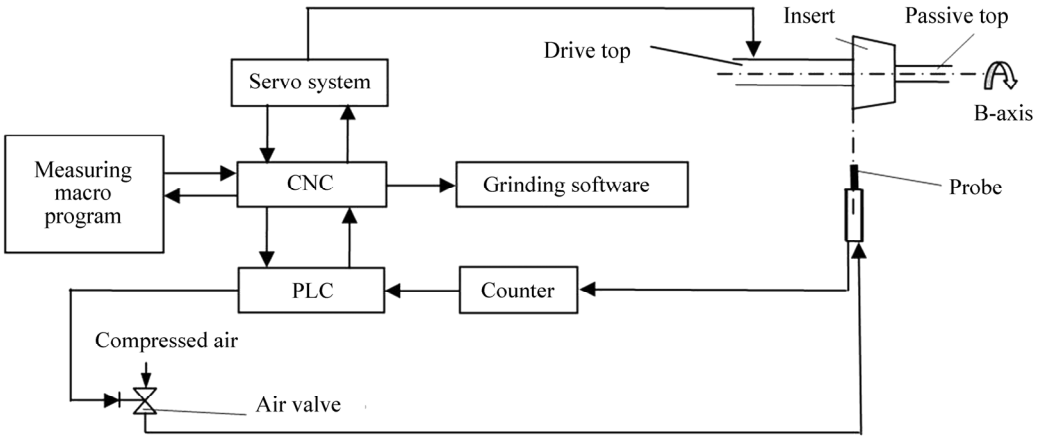

Fig. 9 Structure of online monitoring system

where ξ is a certain percentage, for example ξ=90%. The compensation value x will be input into the offset compensation table of the CNC system as the compensation value in the next grinding circle. The subsequent machining accuracy can be guaranteed in this way. The method of monitoring and compensation proposed above as an integrated approach has a significant advantage that it measures the ground inserts directly instead of measuring the end face of the wheel. Therefore, non-contact displacement sensors, temperature sensors, even large amount of heat-up time can be avoided.

4.3 Experimental verification

In order to verify the feasibility of the dynamic monitoring and automatic error compensation, 300 square carbide inserts are used in the automation grinding experiment. Inscribed circle diameter of each finished insert is measured and the machining accuracy can be gained. The finished size is set to be 15.875 mm and the tolerance requirement is ±0.025 mm. The speed of the wheel is 1500 r/min, and the cooling system works at a supplied air pressure of 1 MPa and delivers approximately 60 L/min of oil. This experiment is completed successfully without any interruption. The dimensions of the finished experiment inserts (Fig. 10) are shown in Fig. 11.

Figure 11 shows that the inscribed circle diameters of experiment inserts are relatively stable, and most deviations are within ±5 μm, far less than the tolerance of ±0.025 mm. The experiment results show that sizes of the finished inserts fluctuate mostly near 15.875 mm, which meets the requirement of machining accuracy.

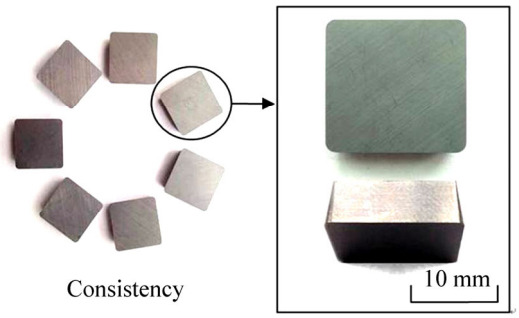

Fig. 10 Part of finished experiment inserts

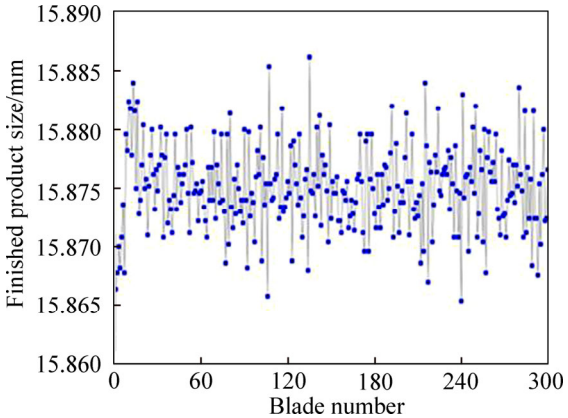

Fig. 11 Dimension of finished experiment inserts

5 Conclusions

1) The structure deformations of the bowl-shaped grinding wheel are investigated based on the centrifugal force. The maximum deformation and maximum stress increase nonlinearly under different rotational speeds.

2) Stress stiffening and spin softening are researched in the structure deformations of the bowl-shaped grinding wheel at different rotation speeds. The results show that deformation influences of stress stiffening are greater than those of spin softening.

3) Theoretical calculation and FEM are used to research the thermal deformation of bowl-shaped grinding wheel caused by grinding heat, and comprehensive analysis of the thermo-mechanical effects on contour structure size of the wheel. The displacement and stress of the wheel increase nonlinearly, and one of the biggest displacement values achieves 248 μm on the grinding wheel face.

4) A method of insert error online dynamic monitoring and automatic compensation is presented. Through the experiment of automatic grinding 300 pieces inserts, the results prove that this method can realize the grinding accuracy requirements.

References

[1] ZHANG Zhe-shan, YAO Bin, ZHANG Xiang-lei, YAO Bo-shi. Accuracy analysis of grinding indexable inserts related to the centrifugal force of high speed abrasive wheel [J]. Advanced Materials Research, 2012, 422: 606−609.

[2] DRAZUMERIC R, BADGER J, KRAJNIK P. Geometric, kinematical and thermal analyses of non-round cylindrical grinding [J]. Journal of Materials Processing Technology, 2014, 214(4): 818−827.

[3] ONISHI T, SAKAKURA M, SATO N, KODANI T, OHASHI K, TSUKAMOTO S. Grinding system reducing the influence of thermal deformation of workpiece in cylindrical grinding [J]. Advanced Materials Research, 2013, 797: 609−612.

[4] MING Xing-zu, YAN Hong-zhi, CHEN Shu-han, ZHONG Jue. 3D models of themo-mechanical coupling of grinding tooth and numerical analysis [J]. Chinese Journal of Mechanical Engineering, 2008, 44(5): 17−24. (in Chinese)

[5] LI Dian-xin, ZHANG Jian-fu, ZHANG Yun-liang, FENG Ping-fa. Modeling, identification and compensation for geometric errors of laser annealing table [J]. Journal of Central South University, 2014, 21: 904−911.

[6] XU Chao, ZHANG Jian-fu, FENG Ping-fa, WU Zhi-jun. Characteristics of stiffness and contact stress distribution of a spindle–holder taper joint under clamping and centrifugal forces [J]. International Journal of Machine Tools and Manufacture, 2014, 82: 21−28.

[7] ZUCCA S, FIRRONE C M, GOLA M M. Numerical assessment of

friction damping at turbine blade root joints by simultaneous calculation of the static and dynamic contact loads [J]. Nonlinear Dynamics, 2012, 67(3): 1943−1955.

[8] LEI Ya-guo, HE Zheng-jia, ZI Yan-yang. EEMD method and WNN for fault diagnosis of locomotive roller bearings [J]. Expert Systems with Applications, 2011, 38(6): 7334−7341.

[9] XIANG Jia-wei, LIU Yi, CHEN Xue-feng, HE Zheng-jia. A wavelet finite element method for the analysis of rotor-bearing systems [J]. Journal of Vibration Engineering, 2009, 22(4): 406−412.

[10] ZHOU Zhen-xin, LI Bei-zhi, YANG Jiang-guo, ZHU Da-hu. Research of chip formation theory in high-speed cylindrical grinding with single grit [J]. Machinery Design & Manufacture, 2011(7): 138−140. (in Chinese)

[11] NI Jun. CNC machine accuracy enhancement through real-time error compensation [J]. Journal of Manufacturing Science and Engineering, 1997, 119(4B): 717−725.

[12] ZHU Shao-wei, DING Guo-fu, QIN Sheng-feng, LEI Jiang, ZHUANG Li, YAN Kai-yin. Integrated geometric error modeling, identification and compensation of CNC machine tools [J]. International Journal of Machine Tools and Manufacture, 2012, 52(1): 24−29.

[13] XU Bing-ye, LIU Xin-sheng. Application of elastic plastic mechanics [M]. Beijing: Tsinghua University Press, 1995: 183−212. (in Chinese)

[14] ZHANG Xiang-lei, YAO Bin, WANG Meng-meng, CHEN Zhan, ZHU Jian. The effect of thermal-mechanical-structure coupling on precision for indexable insert grinded by bowl wheel [J]. Modular Machine Tool and Automatic Manufacturing Techique, 2014(7): 15−18. (in Chinese)

[15] WANG Liu-xin, GUO Ming-yue, GUO Yu. Nature frequency calculation of revolving parts considering stress stiffening and spin softening [J]. Applied Mechanics and Materials, 2013, 427: 33−36.

[16] XIE Gui-zhi, HUANG Han. An experimental investigation of temperature in high speed deep grinding of partially stabilized zirconia [J]. International Journal of Machine Tools and Manufacture, 2008, 48(14): 1562−1568.

[17] SHENG Xiao-ming. Ultra-high speed grinding technology [M]. Beijing: China Machine Press, 2010: 38−40. (in Chinese)

[18] OUTWATER J O, SHAW M C. Surface temperatures in grinding [J]. Trans ASME, 1952, 74: 73−78.

[19] GUO Chang-sheng, MALKIN S. Energy partition and cooling during grinding [J]. Journal of Manufacturing Processes, 2000, 2(3): 151−157.

[20] ZHANG Chao-hui. ANSYS12.0 thermal of engineering practical manual [M]. Beijing: China Railway Publishing House, 2010: 46−52. (in Chinese)

[21] CAO Xiang, YAO Bin, ZHANG Zhe-shan, YAO Bo-shi, LIU Hong-ying. Research on virtual inspection and grinding simulation technology of five-axis CNC tool grinder [J]. Tool Engineering, 2012, 46(9): 119−121.

(Edited by FANG Jing-hua)